Stability of orthoganolly stiffened load-bearing trapezoidal diaphragms

Stability of Orthogonally Stiffened Load-Bearing Trapezoidal Diaphragms

Stabilité de diaphragmes trapézoidaux chargés et raidis rectangulièrement

Stabilität rechteckig ausgesteifter belasteter trapezförmiger Wände

M. A. EL-GAALY

M.S.E., Sc.D., M.ASCE, Senior Engineer, Bechtel Power Corporation,
Ann Arbor, Michigan, USA
Formerly, Lecturer, Department of Civil and Structural Engineering
University College, Cardiff, U.K.

1. Introduction

In box girders, diaphragms are employed to transfer the vertical shear force carried by the webs to the supports. In a previous paper [1], Professor Rockey and the author have considered the problem of stability of unstiffened load bearing trapezoidal diaphragms. It is fully appreciated that most large diaphragms are stiffened and it is the purpose of this paper to develop an approximate method of analysis for uniformly stiffened diaphragms.

In the case of a large number of uniformly spaced stiffeners, one can consider a stiffened plate as a homogeneous orthotropic plate. A survey of the existing literature shows that information is available regarding the buckling of rectangular orthotropic plates with various support conditions and under various cases of loading, however, none is available regarding trapezoidal plates loaded and supported as in load bearing diaphragms. The complexity of the stress distribution in load bearing diaphragms makes an analytical solution impossible and in the present study a numerical method using finite elements has been employed.

The variables in the expression for the buckling load of an orthotropic plate is more than for an isotropic plate, however, in some cases it is possible to combine the variables into the non-dimensional forms K and α in such a way that a single curve of K against α serves to specify the buckling load of an orthotropic plate. Correlation between some stability problems for orthotropic and isotropic plates has been investigated (2–4), and will be advocated in the present study.

2. Stresses in Uniformly Stiffened Diaphragms

The stress distribution which occurs in load bearing trapezoidal diaphragms is complex and depends on various parameters such as the inclination of the webs of the box girder, the aspect ratio of the diaphragm itself and the relative position and width of the supporting pads. Closed form solutions cannot be obtained and it is necessary to resort to numerical methods of analysis. In the present study the finite element method has been used.
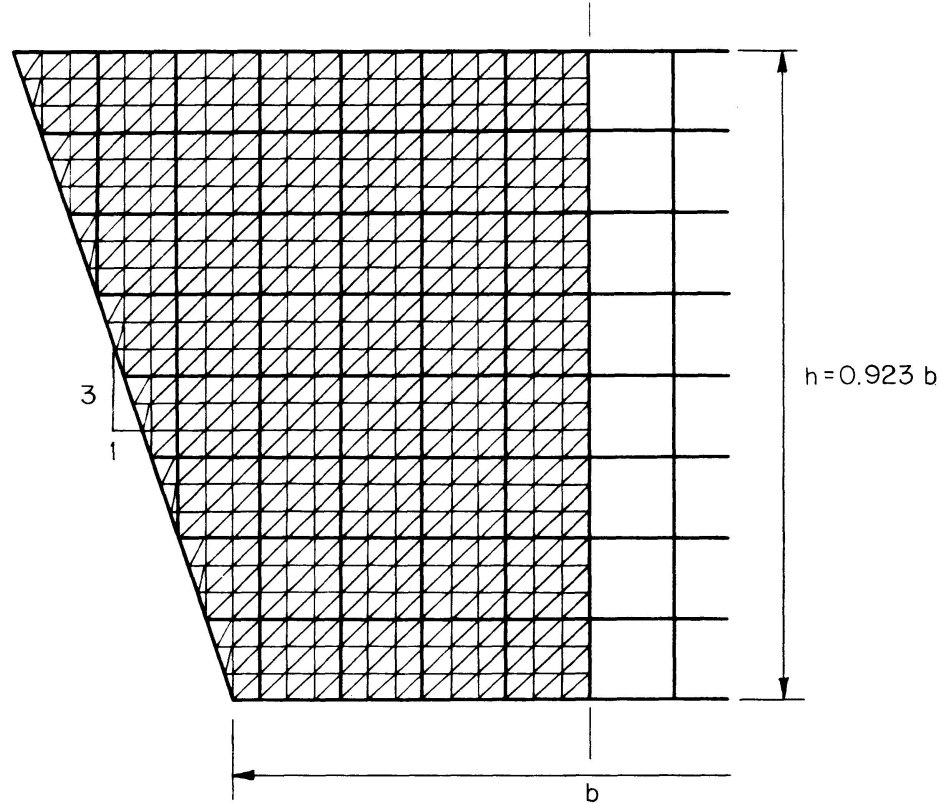
Fig. 1. The finite element idealization.

A possible breakdown of a diaphragm is shown in Fig. 1. As can be noted from the figure and due to symmetry only half the diaphragm needs to be considered. The breakdown of this half consists of 832 plane-stress triangular plate elements and 324 pin ended plane-truss elements intersecting at 458 nodes. In the derivation of the stiffness matrix of the plane stress triangular plate element, the displacements within the element has been represented by the two linear polynomials:

$$u = \alpha_1 + \alpha_2 x + \alpha_3 y$$

and

$$v = \alpha_4 + \alpha_5 x + \alpha_6 y, \tag{1}$$

where u and v are the in-plane displacements in the x and y directions respectively. The full details of the derivation are available in reference [5].

The diaphragm shown in Fig. 1 has been analysed for three possible sup-

porting conditions, namely, a central pad of width $c = 0.23\,b$, two edge pads of width $c = 0.15\,b$ each and a continuous support of the same width as the base of the diaphragm. In all three cases, the supports were assumed to be rigid in the vertical direction but do not prevent horizontal displacements. It has been assumed that the load is transmitted from the webs to the diaphragm by a uniform shear applied along the sides of the diaphragm. The relative area of the siffeners "δ" ($\delta = \frac{A_s}{st}$, where A_s is the area of the stiffener, s is the spacing between the stiffeners and t is the thickness of the plate) has been taken as 0.33 in all three cases, however, in the case of the continuous support relative areas of 0.1 and 0.5 have been considered as well.

The stress distributions obtained were all very similar to the stress distributions for unstiffened diaphragms, which indicates that one can smear the area of the stiffeners over the spacing between them and treat the stiffened diaphragm as if it is unstiffened but with an equivalent thickness,

$$t_e = t(1+\delta).\tag{2}$$

To demonstrate the validity of this assumption the stresses (σ_x, σ_y and τ_{xy}) at various sections calculated for the stiffened diaphragm and the corresponding unstiffened diaphragm with equivalent thickness "t_e" are shown in Fig. 2 for the case of a continuous support and relative area of stiffener, $\delta = 0.33$.

3. Buckling of Rectangular Orthotropic Plates

The general differential equation for the deflection surface of such plates, when submitted to the action of in-plane forces, is

$$D_x \frac{\partial^4 w}{\partial x^4} + 2\,D_{xy} \frac{\partial^4 w}{\partial x^2\,\partial y^2} + D_y \frac{\partial^4 w}{\partial y^4} = -\left[N_x \frac{\partial^2 w}{\partial x^2} + N_y \frac{\partial^2 w}{\partial y^2} + 2\,N_{xy} \frac{\partial^2 w}{\partial x\,\partial y}\right].\tag{3}$$

In this equation,

$$
\begin{aligned}
D_x &= \text{flexural rigidity in the } x\text{-direction,}\\
D_y &= \text{flexural rigidity in the } y\text{-direction,}\\
D_{xy} &= \tfrac{1}{2}(\nu_x D_y + \nu_y D_x) + 2\,(G\,I)_{xy}, \text{ and}\\
2\,(G\,I)_{xy} &= \text{the average torsional rigidity.}
\end{aligned}
$$

In case of *uniform compression* parallel to the x-axis, and for simply supported plate, if the plate buckles into one half-wave, the critical buckling stress can be expressed as follows:

$$\sigma_{cr} = \frac{\pi^2}{b^2 t}\left(D_x \frac{b^2}{a^2} + 2\,D_{xy} + D_y \frac{a^2}{b^2}\right),\tag{4}$$

where
$$
\begin{aligned}
a &= \text{width of the plate,}\\
b &= \text{depth of the plate, and}\\
t &= \text{thickness of the plate, see Fig. 3.}
\end{aligned}
$$
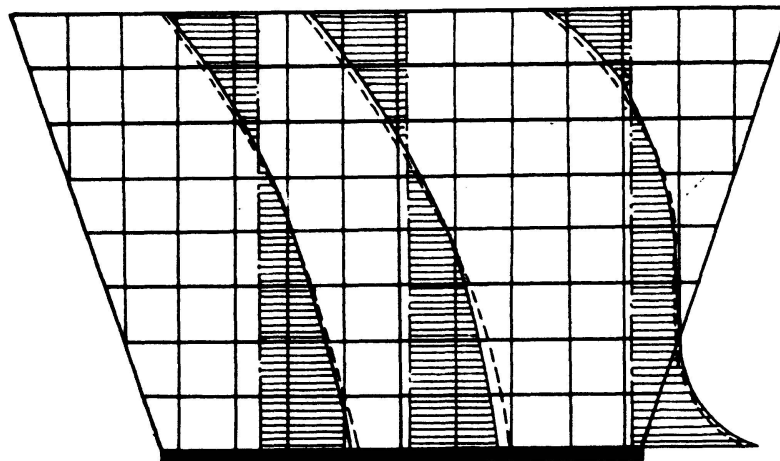
a) Stresses in the x-direction "σ_x".
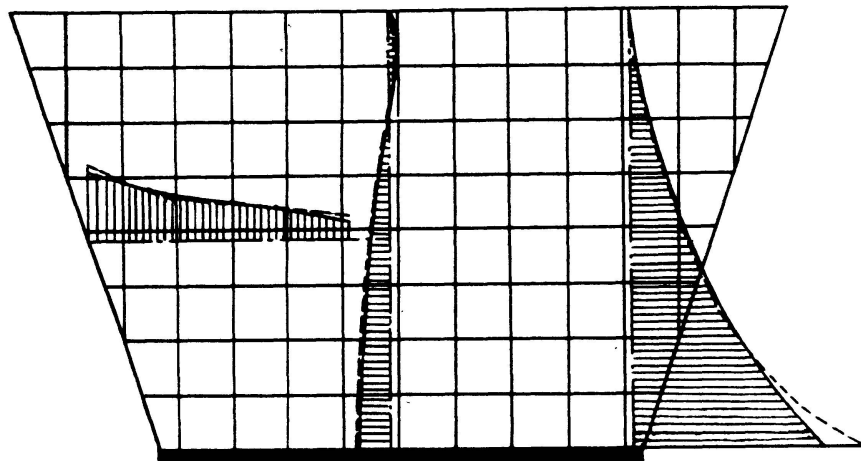
b) Stresses in the y-direction "σ_y".
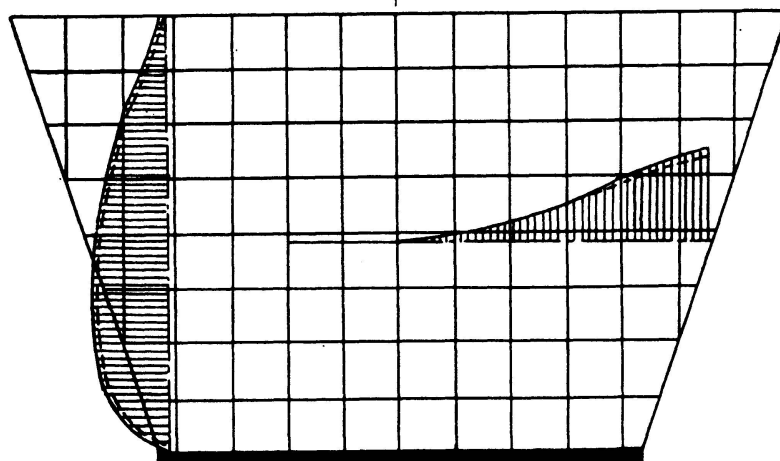
c) Shear stresses "τ_{xy}".

Fig. 2. Comparison between the idealized and actual stresses in the case of a continuous support.

aspect ratio "α" = $\frac{a}{b}$
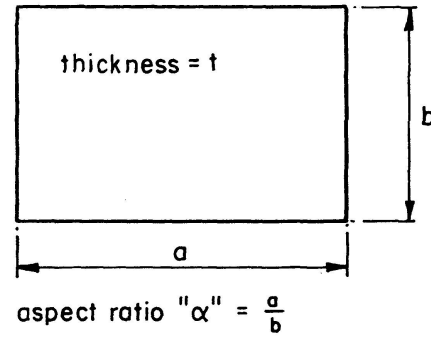
Fig. 3. Dimensions of a rectangular-plate panel. $D = \dfrac{E t^3}{12\,(1 - \nu^2)}$

If the plate buckles into more than one half-wave, say "m" half-waves, then the critical stress can be obtained from Eq. (4) by substituting in it a/m instead of a.

Eq. (4) can be rewritten in the form,

$$\sigma_{cr} = K \frac{\pi^2}{b^2 t} \sqrt{D_x D_y},\tag{5}$$

in which K depends on the parameters

$$\alpha' = \frac{a}{b} \sqrt[4]{\frac{D_y}{D_x}}$$

and

$$\theta = \frac{\sqrt{D_x D_y}}{D_{xy}}.$$

In case of *in-plane bending* applied at the edges parallel to the y-axis, and if the plate buckles into a single half-wave the critical buckling stress can be expressed as follows:

$$\sigma_{1cr} = K \frac{\pi^2}{b^2 t} \sqrt{D_x D_y},\tag{6}$$

in which K depends on the parameters α' and θ as defined before and is given by Eq. (7), namely

$$K = \frac{\pi^2}{16\,\alpha'^2} \left[\frac{\left(1 + \frac{2}{\theta}\alpha'^2 + \alpha'^4\right)\left(1 + \frac{8}{\theta}\alpha'^2 + 16\,\alpha'^4\right)\left(1 + \frac{18}{\theta}\alpha'^2 + 81\,\alpha'^4\right)}{\frac{36}{625}\left(1 + \frac{2}{\theta}\alpha'^2 + \alpha'^4\right) + \frac{4}{81}\left(1 + \frac{18}{\theta}\alpha'^2 + 81\,\alpha'^4\right)} \right].\tag{7}$$

Again if the plate buckles into more than one half-wave, say "m" half-waves, the critical stress can be obtained by substituting in α', a/m instead of a.

When *bending and compression* are combined, the buckling coefficient K can be obtained from the following quadratic in K, namely,

$$\alpha'^4 K^2 \left[\left(\frac{1+\psi}{2}\right)^2 - (1-\psi)^2 \left(\frac{16}{9\pi^2}\right)^2\right] - \alpha'^2 K \left(\frac{1+\psi}{2}\right)\left(2 + \frac{10\alpha'^2}{\theta} + 17\alpha'^4\right)$$

$$+ \left(1 + \frac{2}{\theta}\alpha'^2 + \alpha'^4\right)\left(1 + \frac{8}{\theta}\alpha'^2 + 16\alpha'^4\right) = 0. \tag{8}$$

In the above, ψ = ratio of minimum to maximum stresses,
$(\psi = 1$, for pure compression).

In the case of *pure shear*, the critical shearing stress is given by

$$\tau_{cr} = K\frac{\pi^2}{b^2 t}\sqrt[4]{D_x D_y^3}, \quad \text{for } \theta > 1$$

$$\tag{9}$$

and $\qquad\qquad \tau_{cr} = K\frac{\pi^2}{b^2 t}\sqrt{D_y D_{xy}}, \quad \text{for } \theta < 1,$

where θ is as defined before. Curves of K vs. $1/\alpha'$ for various values of $\theta > 1$ are given in reference (6) for simply supported edges.

4. Buckling of Uniformly Stiffened Rectangular Plates

In the case of a large number of equal and equidistant stiffeners in one direction parallel to one of the sides or in both directions, the stiffened plate can be treated as an orthotropic plate. The values of the stiffness parameters can be evaluated as follows,

$$\begin{aligned} D_x &= D(1+\gamma_x), \\ D_y &= D(1+\gamma_y), \\ D_{xy} &= D, \end{aligned}$$

where D is the flexural rigidity of the plate and γ_x and γ_y are the increase in the flexural rigidity due to the presence of the stiffeners in the x and y directions respectively. In the above it has been assumed that the torsional rigidity of the stiffeners is negligible.

Uniaxial Compression

It can be proved [2] that

$$\sigma_{cro} = \sigma_{cri}\left[\frac{\sqrt{D_x D_y}}{D} + \frac{2}{DK_i}(D_{xy} - \sqrt{D_x D_y})\right], \tag{10}$$

where,

σ_{cro} = critical buckling stress for the orthotropic plate,

σ_{cri} = critical buckling stress for an isotropic plate with an aspect ratio

$\qquad \alpha' = \frac{a}{b}\sqrt[4]{\frac{D_y}{D_x}},$

K_i = buckling coefficient for the isotropic plate, and

D = flexural rigidity for the isotropic plate = $\dfrac{E t^3}{12(1-\nu^2)}$.

If the plate is stiffened in both directions and $\gamma_x = \gamma_y = \gamma$, then Eq. (10) reduces to

$$\sigma_{cro} = \sigma_{cri}(1 + \beta\gamma), \tag{11}$$

where $\beta = 1 - \dfrac{2}{K_i}$, and

σ_{cri} and K_i are for an isotropic plate of an aspect ratio $\alpha' = a/b$.

Meanwhile, if the plate is stiffened in one direction only (the direction of the applied load), then Eq. (10) reduces to

$$\sigma_{cro} = \sigma_{cri}[\sqrt{1+\gamma} + \bar{\beta}(1 - \sqrt{1+\gamma})], \tag{12}$$

where $\bar{\beta} = \dfrac{2}{K_i}$, and

σ_{cri} and K_i are for an isotropic plate of an aspect ratio $\alpha' = \dfrac{a}{b}\dfrac{1}{\sqrt[4]{1+\gamma}}$.

Pure Bending

It is not possible theoretically to prove that Eqs. (11) and (12) are applicable in the case of a plate under pure in-plane bending. However, it can be shown numerically that the relation given by Eqs. (11) and (12) can be used in the case of pure bending with no significant error. Values of β and $\bar{\beta}$ are given in tables 1 and 2 and it can be seen that these values, for all practical purposes, do not vary with γ, however do vary with α' as is expected.

Table 1. Values of β for plates stiffened in two orthogonal directions under pure bending

α	γ					
	1	3	5	10	50	100
0.40	0.612	0.608	0.606	0.605	0.603	0.603
0.50	0.580	0.578	0.577	0.576	0.576	0.575
0.60	0.564	0.564	0.563	0.563	0.563	0.563
0.70	0.561	0.561	0.560	0.560	0.560	0.560
0.80	0.566	0.565	0.565	0.565	0.564	0.564
0.95	0.585	0.583	0.582	0.582	0.581	0.581

Table 2. Values of $\bar{\beta}$ for plates stiffened in one direction only under pure bending

α'	γ					
	1	3	5	10	50	100
0.40	0.386	0.388	0.390	0.391	0.394	0.395
0.50	0.419	0.420	0.421	0.422	0.423	0.424
0.60	0.435	0.436	0.436	0.436	0.437	0.437
0.70	0.439	0.439	0.439	0.439	0.440	0.440
0.80	0.433	0.434	0.434	0.435	0.435	0.435
0.95	0.413	0.415	0.415	0.416	0.418	0.418

Bending and Compression

It has been proved numerically that, again, Eqs. (11) and (12) are applicable when the plate is subjected to in-plane bending and axial compression, tables similar to tables 1 and 2 are available for various values of ψ, from $\psi = -1$ (pure bending) to $\psi = 1$ (pure compression). Representative curves of β and $\bar{\beta}$ vs. α and α' corresponding to various values of ψ are shown in Figs. 4 and 5 for plates stiffened in both directions and in one direction only, respectively.

Table 3. Minimum values of β and $\bar{\beta}$

ψ	β	$\bar{\beta}$	ψ	β	$\bar{\beta}$
-1	0.560	0.439	-0.25	0.509	0.490
-0.9	0.554	0.446	0	0.504	0.496
-0.8	0.549	0.450	0.25	0.501	0.498
-0.7	0.540	0.459	0.5	0.500	0.500
-0.6	0.530	0.468	0.75	0.500	0.500
-0.5	0.522	0.477	1.0	0.500	0.500
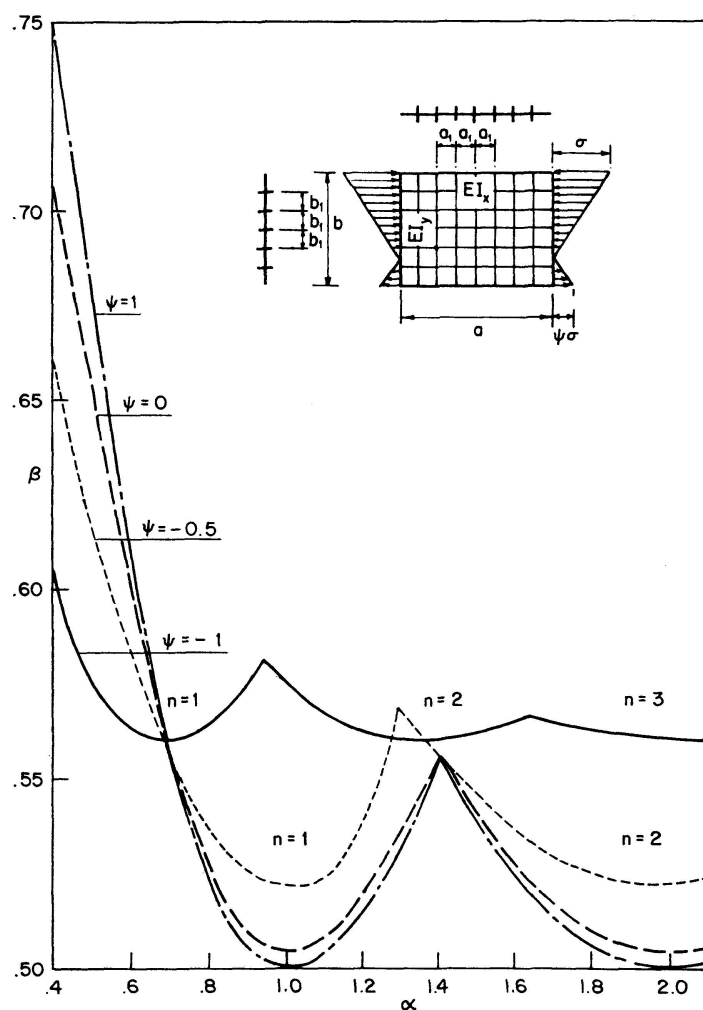
Fig. 4. Values of β vs. α for various values of ψ.
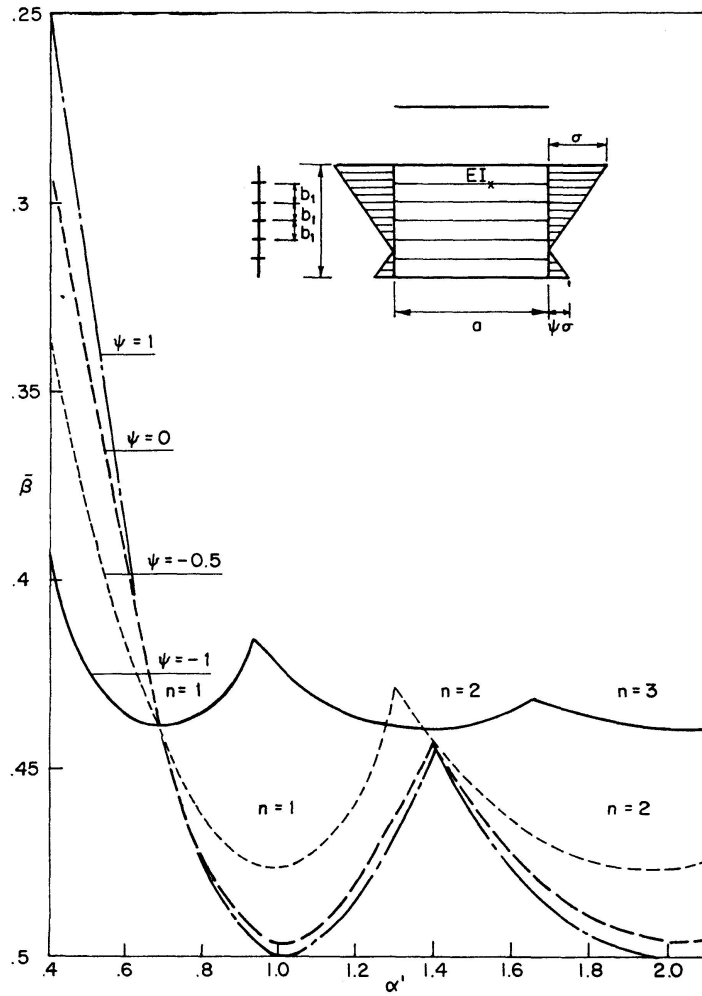
Fig. 5. Values of $\bar{\beta}$ vs. α' for various
values of ψ.

The minimum values of β and $\bar{\beta}$ for various values of ψ are given in table 3 and can be conservatively used.

Shear

The curves of K vs. $1/\alpha'$ for various values of $(1/\theta)$ given in reference [6] are reproduced in Fig. 6, but for K vs. $1/\theta$ and for various values of $1/\alpha'$. It can be seen that for a specific value $1/\alpha'$ and for all practical purposes

$$K = A + B/\theta,\tag{13}$$

where A and B are constants, given in Fig. 6 for various values of $1/\alpha'$.

If the plate is stiffened in both directions and $\gamma_x = \gamma_y = \gamma$, it can be proved that

$$\tau_{cro} = \tau_{cri}\left[\frac{4\,(A+B)}{K_i\,\pi^2} + \frac{4\,A}{K_i\,\pi^2}\gamma\right].\tag{14}$$

But the term $\frac{4\,(A+B)}{K_i\,\pi^2}$ is, for all practical purposes, equal to one as shown in table 4, then Eq. (14) can be written as
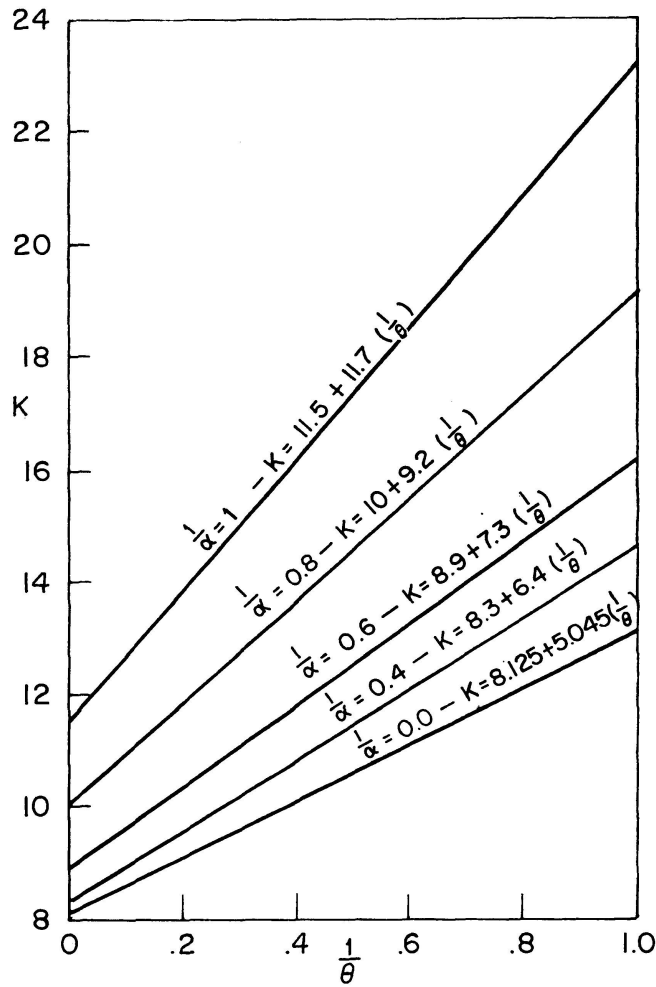
Fig. 6. Values of the buckling coefficient "K" vs. $(1/\theta)$.

Table 4. Values of $\dfrac{4(A+B)}{\pi^2 K_i}$

$\dfrac{1}{\alpha'}$	$\dfrac{4(A+B)}{\pi^2 K_i}$
1.0	1.007
0.8	0.985
0.6	0.968
0.4	0.996
0.0	0.999

$$\tau_{cro} = \tau_{cri}[1 + \beta\gamma], \tag{15}$$

where $\beta = \dfrac{4A}{K_i \pi^2}$,

τ_{cro} = the critical buckling stress for the stiffened plate, and

τ_{cri} and K_i = the critical buckling stress and the buckling coefficient of the unstiffened plate of aspect ratio = b/a.

When the plate is stiffened by transverse stiffeners only, it can be proved that

$$\tau_{cro} = \tau'_{cri}[\sqrt{1+\gamma}+\bar{\beta}(1-\sqrt{1+\gamma})], \tag{16}$$

where
$$\tau'_{cri} = \tau_{cri}\sqrt[4]{1+\gamma},$$

$$\bar{\beta} = \frac{4B}{K_i\,\pi^2}, \text{ and}$$

τ_{cri} and K_i = the critical buckling stress
and the buckling coefficient for the unstiffened plate of
aspect ratio $= \dfrac{b}{a}\dfrac{1}{\sqrt[4]{1+\gamma}}$.

Applications

Comparison between the buckling load values of stiffened plates treated as orthotropic plates and the corresponding available exact values proves that satisfactory results can be obtained by treating the stiffened plate as an orthotropic plate. This is particularly the case when the plate is subjected to compression and/or bending where comparison has been made for a plate reinforced by two equal and equally spaced stiffeners in one direction only (direction of loading), see reference [4]. In the same reference less satisfactory results were obtained for stiffened plates subjected to pure shear.

5. Buckling of Uniformly Stiffened Load-Bearing Trapezoidal Diaphragms

When the diaphragm is uniformly stiffened by large number of horizontal and vertical stiffeners, it is reasonable to assume that the diaphragm will behave as an orthotropic plate. Due to the complexity of the stresses within the area of the diaphragm, a closed form analytical solution is not possible and a numerical method must be used. In this paper the finite element method of analysis was used.
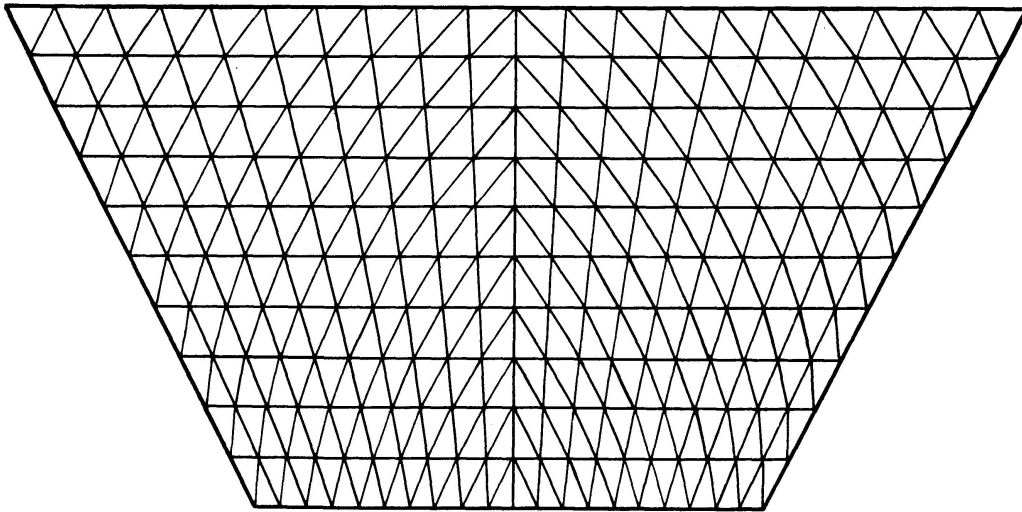

Fig. 7. The finite element idealization.

Fig. 7 shows the finite element idealization as used in the present study. A triangular element with 9 degrees of freedom [7] was used. Full details of the method of analysis will not be given here since it has been reported elsewhere; see references [5], [8], [9] and [10].

The overall buckling load P_{cr} can be expressed as

$$\frac{P_{cr}}{dt} = K \frac{\pi^2 E}{12 (1 - \nu^2)} \left(\frac{t}{d}\right)^2 , \tag{17}$$

in which the non-dimensional parameter K is a function of θ, a/b, c/b, b/d as defined in Fig. 8 and the ratios between D_x, D_y and D_{xy} as defined before. Fig. 9 gives the results obtained for a diaphragm having an aspect ratio $b/d = 1.0$ and which is supported on a non-yielding bearing of width $c = 0.1\,b$. The diaphragm is assumed to be simply supported on all four edges and to be
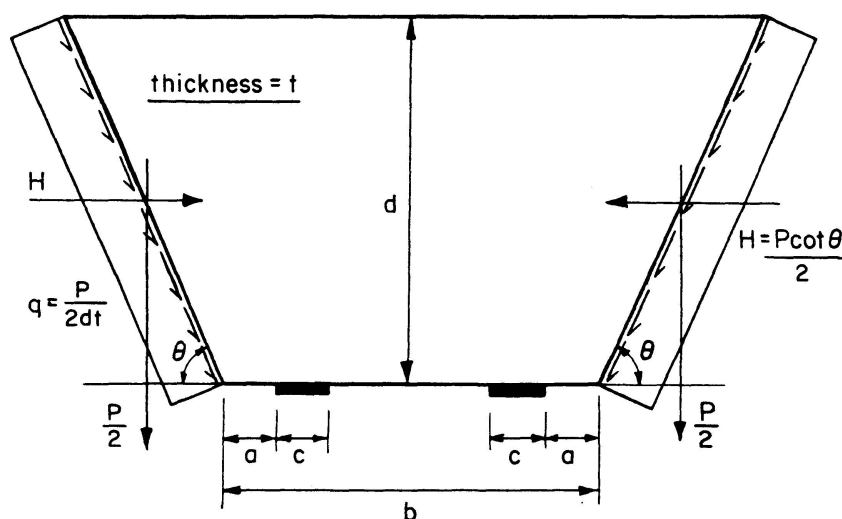

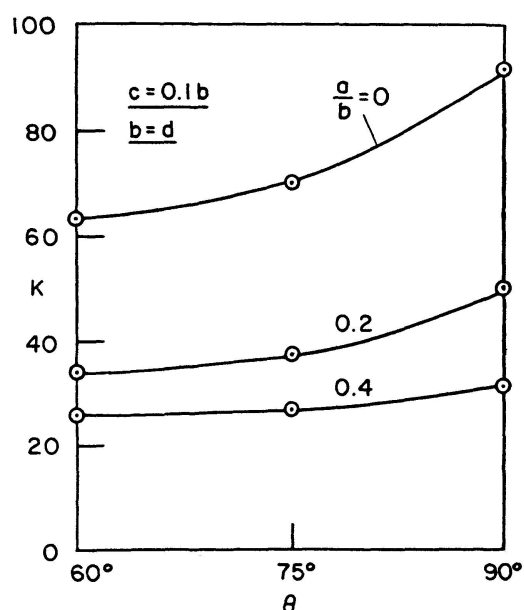Fig. 8. Dimensions and acting forces of a typical diaphragm.

Fig. 9. Buckling load coefficient "K" for various a/b and θ values ($b = d$, $c = 0.1\,b$, $D_x = D_y = 15\,D$, $D_{xy} = D$ and $t_e = t$).
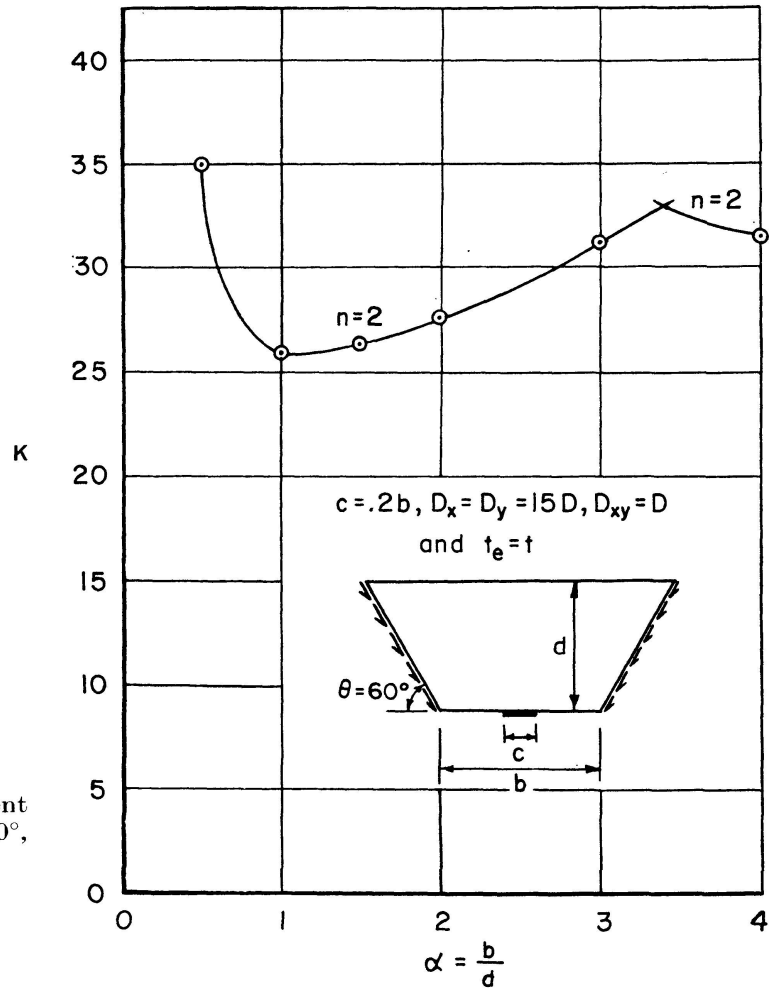
Fig. 10. Buckling load coefficient "K" for various b/d values ($\theta = 60°$, $c/b = 0.2$, $a/b = 0.4$, $D_x = D_y = 15\,D_{xy}$.

subjected to a uniformly applied shear load along its vertical sides. The results given are for the case where $D_x = D_y = 15\,D$, $D_{xy} = D$ and $te = t$; where $D = \dfrac{E\,t^3}{12(1-\nu^2)}$. It will be noted that the variation of the buckling coefficient K with θ and a/b is similar to that for the isotropic diaphragm (1). The variation of the buckling coefficient K with the aspect ratio b/d for a representative case in which the webs are inclined at $60°$ and the central pad has a width of $0.2\,b$ is shown in Fig. 10. It will be noted that the relationship between the buckling coefficient K and the aspect ratio b/d is of a form very similar to that encountered in the isotropic diaphragm [1]. From the above one can conclude that a relationship between the overall buckling load of a uniformly stiffened diaphragm and an isotropic diaphragm exists. This relationship, when the diaphragm is equally stiffened in the x and y directions, can be expressed as before, i.e.

$$P_{cro} = P_{cri}(1 + \beta\gamma),\tag{18}$$

where, P_{cro} is the buckling load for the stiffened diaphragm,

P_{cri} is the buckling load for the unstiffened diaphragm,

and β and γ are as defined before.

When the diaphragm is not stiffened equally in both directions,

$$P_{cro} = P_{cri}\{\sqrt{(1+\gamma_x)(1+\gamma_y)}+\bar{\beta}[1-\sqrt{(1+\gamma_x)(1+\gamma_y)}]\}, \tag{19}$$

where γ_x, γ_y and $\bar{\beta}$ are as defined before and P_{cri} is the buckling load for an isotropic diaphragm of an aspect ratio,

$$\alpha' = \frac{b}{d}\sqrt[4]{\frac{1+\gamma_y}{1+\gamma_x}}. \tag{20}$$

To prove that Eqs. (18) and (19) above are applicable in the case of a trapezoidal diaphragm, values of β for various values of γ are given in table 5 for two diaphragms of aspect ratio $\alpha = 1$ and $\theta = 60°$; one supported by a

Table 5. Values of β for trapezoidal diaphragms of aspect ratio, $b/d = 1.0$ and sides inclination, $\theta = 60°$; stiffened equally in the horizontal and vertical directions

γ	β	
	$\frac{c}{b} = 0.2$, $\frac{a}{b} = 0.4$	$\frac{c}{b} = 0.1$, $\frac{a}{b} = 0$
4	0.637	0.672
9	0.648	0.667
14	0.649	0.667
29	0.650	—
59	0.647	0.667

Table 6. Values of β for trapezoidal diaphragms of aspect ratio, $b/d = 1.0$; stiffened equally in the horizontal and vertical directions

$\frac{c}{b}$	$\frac{a}{b}$	θ		
		90°	75°	60°
0.2	0.4	0.575	0.589	0.649
0.1	0.2	0.555	0.571	0.654
0.1	0	0.530	0.540	0.667

Table 7. Values of β for trapezoidal diaphragms of sides-inclination, $\theta = 60°$ supported by a central pad of width, $c = 0.2\,b$ and stiffened equally in the horizontal and vertical directions

α	β
0.5	0.600
1.0	0.649
1.5	0.700
2.0	0.715
3.0	0.728
4.0	0.657

central pad of width $c = 0.2b$ and the other by two edge pads each of width $c = 0.1b$. As can be noted from the table β, practically, does not vary with γ, however it is different in the two diaphragms, as is expected. Values of β for various cases are shown in tables 6 and 7, from which it can be noted that β is a function of θ, b/d, c/b and a/b.

6. Conclusions

From the study of the stresses in stiffened diaphragms it has been found that it is possible to smear the area of the stiffeners over the spacing between them and treat the stiffened diaphragm as if it is unstiffened but with an equivalent increased thickness.

A correlation between the buckling of uniformly stiffened and isotropic rectangular plates under uniaxial compression and/or in-plane bending and shear has been found. This correlation is applicable to stiffened diaphragms. Using the overall buckling loads for unstiffened diaphragms the overall buckling loads for uniformly stiffened diaphragms can be obtained.

Notation

a	Width of a rectangular plate panel, also distance between the bottom corner of the diaphragm and the outer edge of the supporting pad (see Fig. 8).
A_s	Area of stiffener.
b	Depth of a rectangular plate panel, also width of the bottom edge of the diaphragm.
c	Width of the supporting pad.
d	Depth of the diaphragm.
D	Flexural rigidity of an isotropic plate $\left(= \dfrac{E t^3}{12(1 - \nu^2)} \right)$.
D_x and D_y	Flexural rigidities of an orthotropic plate in the x- and y-directions respectively.
E	Young's modulus of elasticity.
G	Shear modulus or modulus of rigidity.
I	Moment of inertia.
K	Non-dimensional buckling coefficient.
K_i	Buckling coefficient for an isotropic plate.
m	Number of half-waves in the mode of buckling.
P_{cr}	Critical buckling load.
P_{cro} and P_{cri}	Critical buckling loads for the stiffened and unstiffened diaphragms, respectively.
s	Spacing between stiffeners.
t	Thickness of plate.

t_e	Equivalent thickness of plate.
u and v	In-plane displacements in the x- and y-directions, respectively.
α	Aspect ratio of a rectangular plate panel, $\left(= \dfrac{a}{b}\right)$.
γ_x and γ_y	Relative flexural rigidities of stiffeners in the x- and y-directions, respectively.
δ	Relative area of stiffeners $\left(= \dfrac{A_s}{s\,t}\right)$.
θ	Angle of inclination of the web, also a constant as defined in the buckling of orthotropic plates.
τ_{cr}	Critical buckling shearing stress.
τ_{cro} and τ_{cri}	Critical buckling shearing stresses for orthotropic and isotropic plates, respectively.
τ_{xy}	In-plane shear stresses.
ψ	Ratio of minimum to maximum stresses for the case of uniaxial compression and bending ($\psi = 1$ for pure compression and $\psi = -1$ for pure bending).
ν	Poisson's ratio.
ν_x and ν_y	Poisson's ratio in the x- and y-directions, respectively.
σ_{cr}	Critical buckling stress in uniform uniaxial compression.
σ_{1cr}	Critical buckling stress in the case of pure in-plane bending.
σ_{cro} and σ_{cri}	Critical buckling stresses for orthotropic and isotropic plates, respectively.
σ_x and σ_y	Normal stresses in the x- and y-directions, respectively.

References

1. ROCKEY, K. C., and EL-GAALY, M. A.: Stability of load bearing trapezoidal diaphragms. Publication of the I.A.B.S.E., Volume 32-II, p. 155–172, Zurich 1972.
2. WITTRICK, W. H.: Correlation between some stability problems for orthotropic and isotropic plates under bi-axial and uni-axial direct stress. The Aeronautical Quarterly, Volume IV, August 1952, p. 83–92.
3. RICHMOND, B.: Approximate buckling criteria for multi-stiffened rectangular plates under bending and compression. Proceedings of the I.C.E., Vol. 20, 1961, p. 141–150.
4. EL-GAALY, M. A.: Correlation between the buckling of uniformly stiffened and isotropic plates. Report, Civil and Structural Engineering Department, University College, Cardiff, U.K., 1971.
5. ZIENKIEWICZ, O. C.: The Finite Element Method in Structural and Continuum Mechanics. McGraw-Hill, London, 1967.
6. TIMOSHENKO, S. P. and GERE, J. M.: Theory of elastic-stability, second edition. McGraw-Hill Book Company, Inc., 1961.
7. BAZELEY, G. P., CHEUNG, Y. K., IRONS, B. M. and ZIENKIEWICZ, O. C.: Triangular elements in plate bending – conforming and non-conforming solutions. Matrix Methods in Structural Mechanics, Proceedings of the Conference held at Wright-Patterson Air Force Base, Ohio 1965 (Editor J. S. Przemieniecki).
8. KAPUR, K. K., and HARTZ, B. J.: Stability of plates using the finite element method.

Proceedings of the ASCE, Journal of Eng. Mech. Div., Vol. 92, No. EM 2, April 1966, p. 177–195.

9. BAGCHI, D. K.: Large deflection and stability of structural members using the finite element method. Ph. D., thesis, University College, Cardiff, 1969.

10. ROCKEY, K. C., and BAGCHI, D. K.: Buckling of plate girder webs under partial edge loadings. Int. J. Mech. Sci., Pergamon Press 1970, Vol. 12, p. 61–76.

Summary

In this paper, the finite element method of analysis has been used to determine the stress distribution which occurs in uniformly stiffened diaphragms and to determine the applied load at which overall buckling of the diaphragms, treated as orthotropic plates, will occur. It has been found that it is possible to smear the area of the stiffeners over the spacing between them and treat the stiffened diaphragm as if it is unstiffened but with an equivalent increased thickness. A correlation between the buckling of uniformly stiffened plates, treated as orthotropic plates, and isotropic plates has been found; which is applicable to stiffened diaphragms.

Résumé

Dans cet article, on utilise la méthode des éléments finis pour déterminer la répartition des tensions dans des diaphragmes à raidisseurs uniformément répartis, et pour déterminer quelle charge il faut appliquer pour provoquer le voilement des diaphragmes, assimilés à des plaques orthotropes. On arrive à la conclusion qu'il est possible de répartir la surface des raidisseurs sur l'espace qui les sépare et de considérer le diaphragme raidi comme s'il ne possédait pas de raidisseurs, mais une épaisseur plus grande. On trouve une corrélation entre le voilement des plaques à raidisseurs uniformément répartis considérées comme plaques orthotropes, et les plaques isotropes; cela est applicable aux diaphragmes raidis.

Zusammenfassung

In der vorliegenden Arbeit wird die Analyse der endlichen Elementenmethode dazu benützt, um die Spannungsverteilung, die in gleichmässig ausgesteiften Querträgern auftritt, und die angewandte Last zu bestimmen, bei welcher sich allseitiges Beulen der Querträger einstellt, die als orthotrope Platten behandelt werden. Es hat sich gezeigt, dass es möglich ist, die Oberfläche der Aussteifungen über den sie trennenden Raum zu verteilen und den ausgesteiften Querträger als unversteift, aber mit gleichwertiger, vergrösserter Dicke zu behandeln. Es wurde eine Wechselbeziehung zwischen dem Beulen gleichmässig ausgesteifter Platten, die als orthotrope Platten behandelt wurden, und isotropen Platten gefunden, welche auf ausgesteifte Querträger anwendbar ist.

Leere Seite
Blank page
Page vide